THE JOURNAL OF BIOLOGICAL CHEMISTRY VOL. 285, NO. 25, pp. 19184–19192, June 18, 2010

Apobec-1 Complementation Factor Modulates Liver Regeneration by Post-transcriptional Regulation of Interleukin-6 mRNA Stability*[S]

Received for publication, February 17, 2010, and in revised form, April 19, 2010 Published, JBC Papers in Press, April 20, 2010, DOI 10.1074/jbc.M110.115147

Valerie Blanc[‡], Kimberly J. Sessa[‡], Susan Kennedy[‡], Jianyang Luo[‡], and Nicholas O. Davidson[‡§1]

From the Departments of [‡]Medicine and [§]Developmental Biology, Washington University School of Medicine, St. Louis, Missouri 63110

Apobec-1 complementation factor (ACF) is the RNA binding subunit of a core complex that mediates C to U RNA editing of apolipoprotein B (apoB) mRNA. Targeted deletion of the murine *Acf* gene is early embryonic lethal and $Acf^{-/-}$ blastocysts fail to implant and proliferate, suggesting that ACF plays a key role in cell growth and differentiation. Here we demonstrate that heterozygous $Acf^{+/-}$ mice exhibit decreased proliferation and impaired liver mass restitution following partial hepatectomy (PH). To pursue the mechanism of impaired liver regeneration we examined activation of interleukin-6 (IL-6) a key cytokine required for induction of hepatocyte proliferation following PH. Peak induction of hepatic IL-6 mRNA abundance post PH was attenuated >80% in heterozygous $Acf^{+/-}$ mice, along with decreased serum IL-6 levels. IL-6 secretion from isolated Kupffer cells (KC) was 2-fold greater in wild-type compared with heterozygous $Acf^{+/-}$ mice. Recombinant ACF bound an AU-rich region in the IL-6 3′-untranslated region with high affinity and IL-6 mRNA half-life was significantly shorter in KC isolated from $Acf^{+/-}$ mice compared with wild-type controls. These findings suggest that ACF regulates liver regeneration following PH at least in part by controlling the stability of IL-6 mRNA. The results further suggest a new RNA target and an unanticipated physiological function for ACF beyond apoB RNA editing.

Protein-RNA interactions play an important role in post-transcriptional regulation of gene expression, including nuclear mRNA splicing, polyadenylation, and editing as well as cytoplasmic RNA transport, stability, and translation. The protein components required for these various modifications and the pathways involved in their physiological regulation has attracted considerable interest in view of the importance of post-transcriptional modifications in amplifying the genetic repertoire of the host organism (1). Of the two major classes of post-transcriptional RNA editing, C to U RNA editing of mammalian apolipoprotein B (apoB) mRNA has been extensively studied and the minimal core protein components defined (2). ApoB RNA editing is mediated by a multicomponent protein complex with a minimal core containing Apobec-1, the catalytic cytidine deaminase (3) and Apobec-1 complementation factor (ACF),[2] the RNA binding subunit (4, 5). ACF contains three copies of an RNA recognition motif (RRM) identified in other proteins as functioning in protein-RNA interactions and whose modular design and multiplicity likely contribute to refining the specificity and affinity of binding to target RNAs (1). ACF anchors Apobec-1 in an optimal configuration relative to the targeted cytidine within the nuclear apoB RNA and binds with high affinity to an AU-rich region 3′ of the edited base (4, 6).

Although much has been learned about the functional domains in ACF that mediate apoB RNA binding there remain unanswered questions concerning the range of target RNAs and cell-specific factors that influence ACF-RNA binding and its physiological consequences. Questions concerning potential RNA targets were first raised with the demonstration that ACF is expressed in tissues that do not express apoB RNA (4, 5, 7) and assumed greater significance with the surprising finding that germline deletion of murine *Acf* resulted in early embryonic lethality (8). These observations, coupled with the finding that ACF is expressed at high levels in human and mouse liver (8), suggested the possibility that a loss-of-function phenotype might be elicited in the liver of adult $Acf^{+/-}$ (heterozygous knock-out) mice.

The liver has a unique yet incompletely understood capacity for regeneration following either injury or surgical resection. The process of liver regeneration following partial hepatectomy (PH) is initiated within hours and orchestrated by distinct signaling cascades involving cytokines and growth factors as well as *Wnt*-dependent pathways that together direct genetic programs that lead to hepatocyte re-entry into and progression through the cell cycle (reviewed in Refs. 9–11). Interleukin-6 (IL-6) is among the key cytokines involved in liver regeneration as evidenced by studies demonstrating hepatic necrosis and liver failure in IL-6 knock-out mice following PH (12). IL-6 mRNA is unstable and contains elements in the 3′-untranslated region (UTR) that confer instability and rapid turnover of a

* This work was supported, in whole or in part, by National Institutes of Health Grants HL-38180, DK-56260, and DK-52574 (to N. O. D.) and American Heart Association Graduate Student Fellowship 910115 (to K. J. S.).

[S] The on-line version of this article (available at http://www.jbc.org) contains supplemental Fig. S1.

[1] To whom correspondence should be addressed: Div. of Gastroenterology, Box 8124, Washington University School of Medicine, 660 Euclid Ave., St. Louis, MO 63110. E-mail: nod@wustl.edu.

[2] The abbreviations used are: ACF, Apobec-1 complementation factor; PH, partial hepatectomy; IL-6, interleukin-6; 3′-UTR, 3′-untranslated region; KC, Kupffer cell; PBS, phosphate-buffered saline; Q-PCR, quantitative PCR; MEF, mouse embryonic fibroblast; CLIP, cross-linking and immunoprecipitation; LPS, lipopolysaccharide; RRM, RNA recognition motif; STAT, signal transducers and activators of transcription; nt, nucleotide.

reporter RNA expressed in heterologous cells (13). We now demonstrate defective hepatic regeneration in $Acf^{+/-}$ mice with decreased IL-6 induction and further show that ACF binds to instability elements in the IL-6 3′-UTR. In addition, we demonstrate that IL-6 mRNA turnover is accelerated in Kupffer cells isolated from $Acf^{+/-}$ mice. The findings collectively suggest a new RNA target and expanded the functional role for ACF.

MATERIALS AND METHODS

Animals—In view of the early embryonic lethality associated with germline *Acf* deletion, we used $Acf^{+/-}$ mice maintained in a mixed 129sv/J X C57BL/6J background (8) and fed standard chow diet. All experiments were approved by the Animal Studies Committee of Washington University (number 20070022) and performed according to the institutional guidelines. Eight-week-old mice underwent 70% partial hepatectomy or sham surgery under isoflurane anesthesia as previously described (14). Mice were injected intraperitoneally with 100 mg/kg of bromodeoxyuridine (Sigma) 2 h before sacrifice. At various times after surgery, animals were sacrificed, weighed, and the liver fixed in 10% formalin for 24 h for histological staining. Paraffin-embedded sections of liver were stained for bromodeoxyuridine, using a mouse monoclonal anti-BrdUrd antibody (DAKO, CA) followed by horseradish peroxidase-linked anti-mouse IgG. For each animal, three to five random ×400 fields were examined and 300–400 nuclei were counted to evaluate BrdUrd staining (14). Serum IL-6 was determined using eBioscience recombinant mouse interleukin-6, affinity purified, and Biotin anti-mouse IL-6, following the manufacturer's protocol (eBioscience).

Kupffer Cell (KC) Isolation—Three to four mice of each genotype were used for each isolation as described (15). Briefly, livers were perfused in calcium and magnesium-free HEPES-buffered sterile saline and then digested with collagenase (type IV) (Sigma). Non-parenchymal cells were separated from the hepatocytes by two consecutive centrifugations at 50 × *g*. The supernatant was then centrifuged at 800 × *g* for 10 min. The non-parenchymal cell-enriched pellet was layered on top of a 25–50% Percoll gradient and centrifuged at 800 × *g* for 15 min. The KC-enriched fraction was collected, washed in PBS, and positively selected using biotin-conjugated anti-mouse CD115 (eBioscience), biotin-conjugated anti-F4/80 (Cedarlane), and magnetic MicroBeads following the manufacturer's protocol (Miltenyi Biotec). Identity of isolated Kupffer cells was confirmed by Q-PCR (see below) of a Kupffer cell-specific receptor (C-type lectin type 4) (16) using the following primers: forward KC-receptor, 5′-GGCAGCAGTGGAATGACATG-3′; reverse FC-receptor, 5′-CACCCTGTGGACTTCTTGCA-3′. Purified KCs were cultured in RPMI 1640 medium supplemented with 10% fetal bovine serum for 12 h. Medium was collected and IL-6 concentration was determined by enzyme-linked immunosorbent assay as described above. RNA was isolated with TRIzol (Invitrogen) and IL-6 mRNA was analyzed by quantitative and semi-quantitative PCR. Where indicated in the figure legends, isolated KCs were stimulated for 1 h with 500 ng/ml of lipopolysaccharide (LPS, Sigma L4391) prior to washing, addition of actinomycin D (10 μg/ml) (Sigma), and RNA extraction at the indicated times. For immunofluorescence studies, KCs were seeded on glass coverslips for 12 h, fixed with 10% formalin, and co-stained with rabbit anti-ACF (6) and mouse anti-F4/80 (Cedarlane) followed by fluorescent secondary antibodies.

Mouse Embryonic Fibroblast (MEF) Isolation—Three to four mice per genotype were used to isolate MEFs as described (17). Briefly, embryos were isolated from uteri of 13.5-day pregnant mice, digested in trypsin/EDTA, and dissociated. The cell pellets were resuspended in 10 ml of growth medium (Dulbecco's modified Eagle's medium, 10% fetal bovine serum, 1% glutamine, 1% nonessential amino acids, penicillin, streptomycin), and seeded on 60-mm dishes.

RNA Extraction and Real Time Q-PCR—Total RNA was extracted from snap-frozen mouse liver (~100 mg) and DNase-treated RNA (2 μg) was reverse-transcribed and Q-PCR performed with an ABI Prism 7000 instrument (Applied Biosystems) using SYBR Green Master Mix according to the manufacturer's instructions. mRNA abundance was normalized to 18 S RNA in each sample. PCR primers were as follows: IL-6 forward, 5′-CTTCCTACCCCAATTTCCA-ATG-3′, reverse 5′-ATTGGATGGTCTTGGTCCTTAGC-3′; 18S, forward 5′-GCTGGAATTACCGCGGCT-3′, reverse 5′-CGGCTACCACATCCAAGGAA-3′.

Protein Extraction and Western Blot—Liver extracts were homogenized in tissue lysis buffer (20 mM Tris, pH 8.0, 150 mM NaCl, 2 mM EDTA, 1% Triton, 0.1% SDS, 100 mM NaF, 1 mM $NaVO_3$, 50 mM β-glycerophosphate, 5% glycerol and protease inhibitors (Roche Applied Science)). Samples were pelleted by centrifugation at 14,000 × *g* and aliquots (100 μg of protein) were separated by SDS-10% PAGE. After transfer, the membrane was incubated with antibodies against phospho-STAT3 (Tyr^{705}) (Cell signaling Technology) at a 1:2000 dilution following the manufacturer's protocol followed by secondary anti-mouse IgG (GE Healthcare) at a 1:5000 dilution. Bands were revealed using ECL reagent (GE Healthcare).

Cloning of IL-6 3′-UTR—IL-6 full-length 3′-UTR was amplified from mouse liver cDNA and cloned into pcDNA3 (Invitrogen) using HindIII and BamHI restriction sites to generate pCDNA3 (IL-6 FL-UTR) plasmid. The primers used to amplify the full-length 3′-UTR are as follows: forward, 5′-GGTGGTT-CTAGAAAGCTTTGCGTTATGCCTAAGCATATCAGTT-TGTGG-3′, reverse, 5′-GGTGGTTCTAGAGGATCCGAAG-ACAGTCTAAACATTATAAAAATAC-3′. This recombinant plasmid was used as template to amplify the 128-bp AU-rich sequence spanning from nucleotides 112 to 240 (nucleotide 1, being the first nucleotide of the untranslated sequence). Mutant 1 and Mutant 2 were generated by the two-step PCR method (6) using the following primers: Mutant 1: primer set 1, IL-6 3′UTRmut1-Fwd, 5′-GGGACACTATTTTAATTATTT-TTAACTGCTTGATAGTCTGAATAAGTAAAC-3′; mIL-6 3′UTR-Rev, 5′-GGTGGTTCTAGAGGATCCAAACTATAA-CATATAACATTTCAAGTGACAC-3′; mIL-6 3′UTR-Fwd, 5′-GGTGGTTCTAGAAAGCTTGAATGTTGGGACACTA-TTTTAATTATTTTT-3′; IL-6 3′UTRmut1-Rev, 5′-GTTTA-CTTATTCAGACTATCAAGCAGTTAAAAATAATTAAA-ATAGTGTCCC-3′ Mutant 2: primer set 1: mIL-6 3′UTR-Fwd and IL-6 3′UTRmut2-Rev, 5′-CTTCATAAAAATAATGCAG-

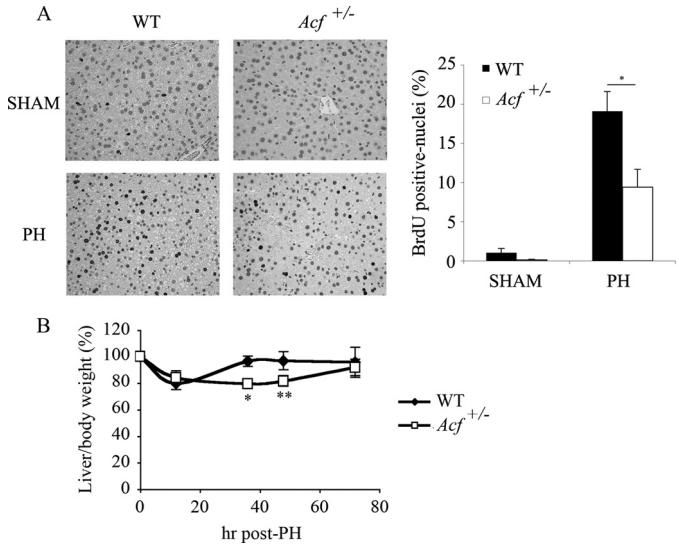

FIGURE 1. **Impaired liver regeneration in $Acf^{+/-}$ mice after partial hepatectomy.** *A*, *left panel*, sections from wild type and $Acf^{+/-}$ mice livers harvested 48 h after partial hepatectomy and stained for BrdUrd incorporation. *Right panel*, percentage of hepatocytes labeled with BrdUrd 48 h following partial hepatectomy in wild type and $Acf^{+/-}$ mice (6–8 animals per genotype; *, $p < 0.05$). *B*, reduced liver to body weight ratio in $Acf^{+/-}$ mice following PH. Wild type and $Acf^{+/-}$ animals were weighed and sacrificed 12, 36, 48, and 72 h after PH and liver weights recorded. Data show the liver to body weight ratio, normalized to the starting liver to body weight ratio values (5.8% liver weight/body weight for WT animals *versus* 5.4% for $Acf^{+/-}$ mice). Data are from four to five animals per genotype, per time point; *, $p < 0.05$; **, $p < 0.01$.

ATCAATCACAGACTAACTTAAAG-3′; IL-6 3′UTRmut2-Fwd, 5′-CTTTAAGTTAGTCTGTGATTGATCTGCATTA-TTTTTATGAAG-3′ and mIL-6 3′UTR-Rev. Primer set 2 for both mutants was mIL-6 3′UTR-Fwd and mIL-6 3′UTR-Rev. Recombinant pcDNA3 constructs were used to generate RNA *in vitro* using T7 RNA polymerase and [^{32}P]UTP.

IL-6 mRNA Splicing—IL-6 RNA splice forms were analyzed using reverse transcriptase-PCR on mouse liver RNA as described (18). Two rounds of nested PCR were performed using the following primers: round 1, primer U3 5′-GAGCCCAC-CAAGAACGATAGTC-3′ and primer R1 5′-ATTAAAAA-TAATTAAAATAGTGTCCCAAC-3′; round 2, primer U1 5′-CGCTATGAAGTTCCTCTCTGC-3′ and primer R3 5′-CTAGGTTTGCCGAGTAGATCTC-3′. PCR products (5 μl) were separated on a 1.8% agarose gel and visualized under UV light.

Protein-RNA Interaction, UV Cross-link, and Filter Binding Assay—^{32}P-Labeled mouse IL-6 3′-UTR RNA (50,000 cpm) was incubated with recombinant ACF for 15 min at room temperature in 10 μl of binding buffer containing 10 mM HEPES, pH 8.0, 100 mM KCl, 1 mM EDTA, 0.25 mM dithiothreitol, and 2.5% glycerol. The RNA was treated with heparin (2 mg/ml final concentration) (Sigma) and RNase T1 (Sigma) (2 units/μl) prior to UV irradiation on ice in a Stratalinker (Stratagene) at 250 mJ/cm^2. The cross-linked material was analyzed by 10% SDS-PAGE and visualized by autoradiography. RNA binding competition assays were performed by co-incubating ACF with radiolabeled AU-rich probe and unlabeled AU-rich, rat apoB RNA (nucleotides 6639–6743, flanking the edited base), and p21 coding region considered as a non-AU RNA template.

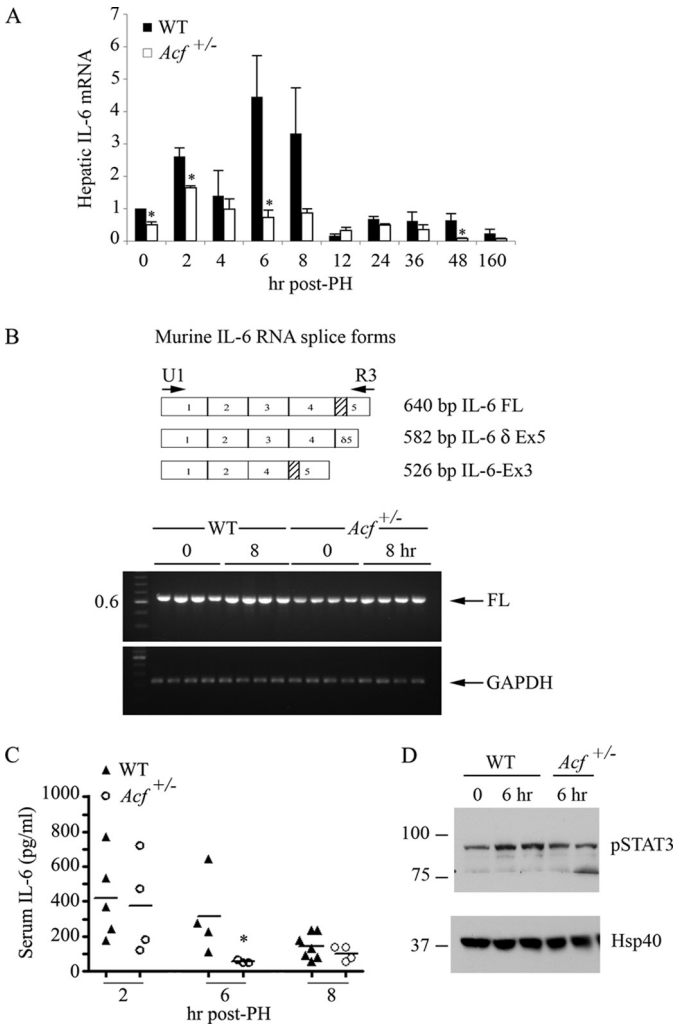

FIGURE 2. **Altered IL-6 gene expression profile during liver regeneration in $Acf^{+/-}$ mice.** *A*, wild-type and $Acf^{+/-}$ mice were sacrificed at the indicated times following PH and RNA extracted. Expression profile of IL-6 mRNA (individual samples) was analyzed by quantitative reverse transcription-PCR. Data were standardized to the expression of 18 S mRNA (n = 3–8 animals per genotype and time point; *, $p < 0.05$). *B*, *top panel*, scheme of alternative splicing of murine IL-6 RNA. *Shaded box* indicates the deleted region resulting from alternative splicing of exon 5. *Lower panel*, IL-6 reverse transcription-PCR profile from WT and $Acf^{+/-}$ mice at 0 and 8 h following liver resection. Specific primers U1 and R3 (see "Materials and Methods" and panel) were used to co-amplify the three IL-6 spliced forms. PCR products were separated on a 1.8% agarose gel and visualized by ethidium bromide under UV light. cDNAs from 4 animals per genotype and per condition were analyzed. Only the full-length (*FL*) form of IL-6 RNA was detected. *GAPDH* (glyceraldehyde-3-phosphate dehydrogenase) mRNA was amplified and used as control. *C*, reduced serum IL-6 in $Acf^{+/-}$ mice. Serum was collected at the indicated times following PH and serum IL-6 was analyzed by enzyme-linked immunosorbent assay. *D*, STAT3 activation after partial hepatectomy. Phosphorylated STAT3 protein was analyzed by Western blot in liver extracts from WT and $Acf^{+/-}$ that were sacrificed 6 h after liver resection. Hsp40 was used as loading control.

Binding efficiency was determined by phosphorimaging (GE Healthcare). Filter binding assays were performed using 2 ng of radiolabeled IL-6 full-length 3′-UTR and increasing concentrations of recombinant ACF in a 10-μl reaction as described for the UV cross-link assay. Following the heparin and RNase T1 incubation, the binding reactions were loaded on 0.45-μm nitrocellulose filters (Millipore). After three consecutive washes with binding buffer (8 ml/wash/filter), filters were dried and bound RNA counts were determined using a liquid scintil-

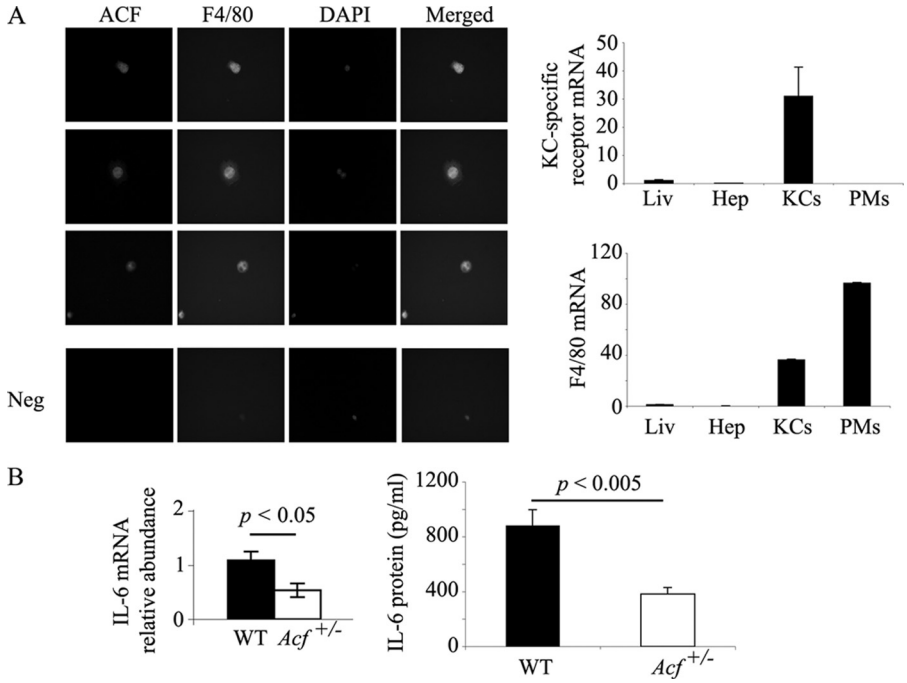

FIGURE 3. **ACF expression in Kupffer cells modulates IL-6 production.** *A*, *left panel*, purified Kupffer cells were seeded on coverslips overnight and co-stained with rabbit anti-ACF IgG, and mouse F4/80. 4′,6-Diamidino-2-phenylindole staining indicates the nucleus. This is a representative of two independent assays. Here are shown three separate fields. *Right panels*, Kupffer cell specific-receptor mRNA and F4/80 mRNA expression in liver (*Liv*), hepatocytes (*Hep*), Kupffer cells (*KCs*), and mouse peritoneal macrophages (*PMs*) were analyzed by Q-PCR. Data were standardized to 18 S RNA. Data represent mean ± S.E. (n = 3–5 RNA isolations per cell type or tissue). *B*, Kupffer cells, isolated from WT and $Acf^{+/-}$ mice, were grown overnight at 37 °C. Medium and RNA were collected for IL-6 RNA and protein analyses. IL-6 RNA was analyzed by Q-PCR. 18 S RNA was used to standardize the data. Data represent mean ± S.E. (n = 4–5 Kupffer cell isolations per genotype). KC medium was used in an enzyme-linked immunosorbent assay for IL-6 quantitation, the data represent mean ± S.E. (n = 3 Kupffer cell isolations per genotype).

lation counter. Reactions performed without recombinant ACF were used to evaluate background. After background deduction, bound RNA was expressed as percentage of input RNA.

In Vivo Cross-linking and Immunoprecipitation (CLIP)—RAW 264.7 cells were maintained in Dulbecco's modified Eagle's medium (Invitrogen) and treated with 100 ng/ml of lipopolysaccharide (LPS) (Sigma) for 24 h at 37 °C. RAW cells and, where indicated, murine liver extracts were used in CLIP assays, which were performed with minor modifications as detailed below from the original method (19). Cells were exposed to 300 mJ cm^2 UV irradiation in a Stratalinker and collected in 1× PBS. The cell pellets were lysed in PLB buffer (10 mM HEPES, pH 8, 100 mM KCl, 5 mM $MgCl_2$, 10 mM ribonucleoside vanadyl complexes (Sigma), 0.5% Nonidet P-40, 1 mM dithiothreitol, 0.2 mM phenylmethylsulfonyl fluoride and protease inhibitors (Roche)). Cell lysates were centrifuged twice at 14,000 × *g*, 10 min each. The supernatant (1 mg) was pre-cleared with 100 μl of pre-swollen magnetic Dynabeads protein A beads (Invitrogen). The supernatant was divided into three fractions: 100 μl was directly extracted with TRizol and represents input RNA. The two other fractions (750 μl each) were incubated overnight with either protein A beads coupled to anti-ACF antibody (25 μg) or to unrelated rabbit IgG in NT2 buffer (50 mM Tris, pH 7.4, 150 mM NaCl, 1 mM $MgCl_2$, 0.05% Nonidet P-40) supplemented with 200 units of RNase inhibitor (Invitrogen), 2% ribonucleoside vanadyl complexes, 1 mM dithiothreitol, 150 mM EDTA. The beads were washed twice in Buffer A (1× PBS (no Mg^{2+}, no Ca^{2+}), 0.1% SDS, 0.5% deoxycholate, 0.5% Nonidet P-40), twice in Buffer B (5× PBS (no Mg^{2+}, no Ca^{2+}), 0.1% SDS, 0.5% deoxycholate, 0.5% Nonidet P-40), and twice in Buffer C (50 mM Tris, pH 7.4,10 mM $MgCl_2$, 0.5% Nonidet P-40). Beads were resuspended in 100 μl of NT2 buffer supplemented with 0.1% SDS, 80 units of RNase OUT (Promega), 30 μg of proteinase K (Sigma), and incubated 30 min at 55 °C. RNA was extracted and the immunoprecipitated purified RNA used for cDNA synthesis followed by PCR for IL-6 detection. Murine IL-6-specific primers: mIL-6 UTR-Fwd, 5′-GGTGGTGGATCCGAATGTTGGGACAC-3′ and mIL-6 UTR-Rev, 5′-AAACTATAACATATAACATTTCAAGTGACAC-3′; and murine albumin-specific primers: mAlb 411-Fwd, 5′-ACCATTTGAAAGGCCAGAGGC-3′; mAlb 742-Rev, 5′-GGAATGTCTGGCTCAGACGAAC-3′; and murine apoB-Fwd, 5′-ATCTGACTGGGAGAGACAAGTAG-3′, rev, 5′-CACGGATATGATACTGTTCGTCAAGG-3′ were used.

Statistical Methods—The data are presented as mean ± S.E. with all statistical comparisons using paired Student's t tests with GraphPad Prism (version 4.03, San Diego, CA) and Microsoft Excel 2004.

RESULTS

Decreased Proliferation and Delayed Liver Regeneration in $Acf^{+/-}$ Mice following PH—To begin addressing the role of ACF in liver growth and proliferation, we examined hepatocyte proliferation after PH in wild-type and $Acf^{+/-}$ mice. These findings (Fig. 1*A*) revealed a 50% decrease in hepatic proliferation in $Acf^{+/-}$ mice at 48 h, which corresponds to completion of the first round of hepatocellular DNA synthesis and peak mitotic progression during liver regeneration (11). A significant delay was also evident in liver mass recovery in $Acf^{+/-}$ mice where complete restitution required 72 h compared with 48 h in controls (Fig. 1*B*).

Defective Induction of IL-6 Gene Expression in $Acf^{+/-}$ Mice following PH—Considerable evidence suggests that cytokines including tumor necrosis factor α and IL-6 play an important role in liver regeneration following PH at least in part through their actions on early priming events prior to reentry into the cell cycle, with induction of gene expression noted within the first few hours (9–11). To explore the possibility that the delayed proliferative response in $Acf^{+/-}$ mice reflected alterations in the production of one of these candidate cytokines, we undertook RNA profiling of livers at various times following

PH. The results revealed the expected increase in hepatic IL-6 mRNA abundance (Fig. 2*A*) in wild-type animals, with a peak at 6 h. By contrast, despite a brief induction at 2 h, there was no sustained induction of IL-6 mRNA in $Acf^{+/-}$ mice (Fig. 2*A*). We entertained the possibility that changes in hepatic IL-6 mRNA expression in $Acf^{+/-}$ mice might involve differential alternative splicing, similar to what has been observed in other murine tissues (20). However, this was not the case. In all samples analyzed, the dominant form of IL-6 mRNA was the full-length transcript (Fig. 2*B*). In keeping with the hepatic RNA data, serum IL-6 was increased in both genotypes at 2 h post-PH, with an early decline at 6 h noted in $Acf^{+/-}$ mice (Fig. 2*C*). These findings were extended by examining the activation of STAT3 as a surrogate indicator of IL-6 signaling, which showed that activation/phosphorylation of STAT3 following PH was attenuated in $Acf^{+/-}$ mice 6 h following PH (Fig. 2*D*).

Decreased Secretion of IL-6 from Kupffer Cells in $Acf^{+/-}$ Mice—Analysis of Kupffer cells isolated from wild-type mice demonstrated a superimposable pattern of immunofluorescence staining for both ACF and F4/80 (Fig. 3*A*). These findings suggest that ACF is expressed in hepatic non-parenchymal cells, which are likely a dominant source of IL-6 production (21). To exclude the possibility that staining for F4/80 reflected contamination with peripheral macrophages, we verified expression of the KC-specific C-type 4 lectin (16) in our preparations of KCs but not from peritoneal macrophages (Fig. 3*A*, *right panel*). We further demonstrated that IL-6 mRNA abundance and secretion were both significantly reduced in KC isolated from $Acf^{+/-}$ mice compared with wild-type animals (Fig. 3*B*). These findings collectively indicate that ACF is expressed in KC and that reduced ACF expression (in $Acf^{+/-}$ mice) is associated with attenuated IL-6 gene expression.

ACF Binds to the 3′-UTR of IL-6 mRNA—The findings to this point suggest that reduced levels of hepatic ACF are associated with delayed liver regeneration and reduced production of IL-6. However, in view of the affinity of ACF for AU-rich targets (such as the region of apoB mRNA flanking the edited base (4, 6)) and the importance of post-transcriptional regulation of IL-6 mRNA turnover, we examined the possibility that ACF binds target regions within the 3′-UTR, particularly those known to harbor conserved AUUUA motifs (Fig. 4*A*). UV cross-linking revealed binding of recombinant ACF to the full-length IL-6

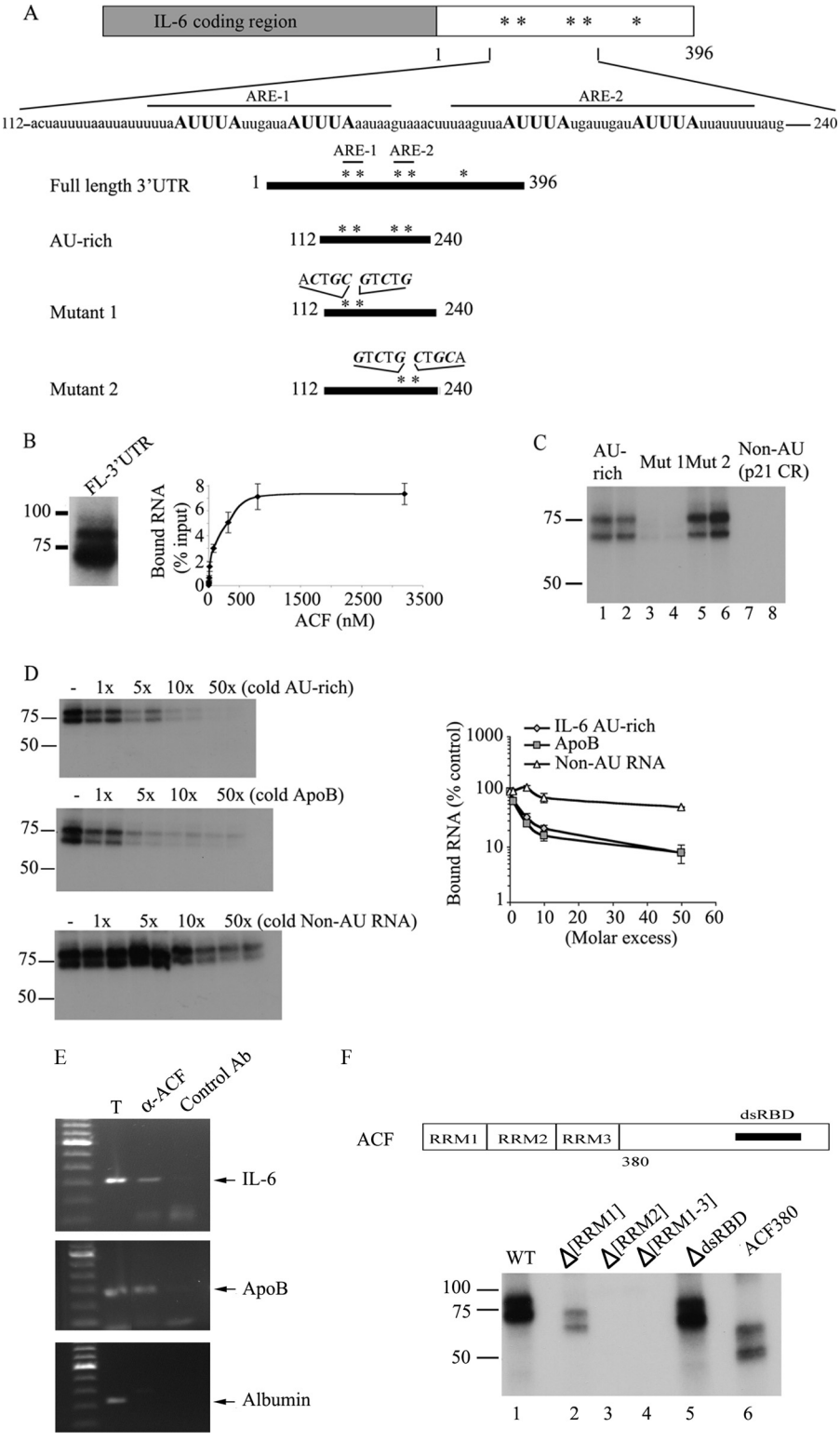

3′-UTR (Fig. 4*B*). Filter binding assays indicated that ACF binds IL-6 3′-UTR in a saturable manner with an apparent K_d of ~100 nM (Fig. 4*B*), a value similar to that for ACF binding to apoB RNA (~200 nM, data not shown). ACF also interacts with a 128-nt AU-rich region containing four clusters of AUUUA motifs (Fig. 4*C*). We further refined the binding of ACF requirements within this 128-nt AU-rich fragment by introducing point mutations into either the proximal or distal pairs of AUUUA motifs (Fig. 4, *A* and *C*). UV cross-linking revealed that mutation of the proximal pair of AUUUA motifs (mutant 1) eliminated ACF binding, whereas binding to mutant 2 was unimpaired (Fig. 4*C*). Similarly, ACF failed to bind a non-AU template, supporting ACF requirements for AU-rich motifs (Fig. 4*C*). The specificity of RNA binding was verified in a competition assay using either the cold unlabeled AU-rich fragment itself (Fig. 4*D*, *top left panel*) or cold unlabeled apoB RNA, a similar sized (105 nt) AU-rich fragment flanking the edited base (Fig. 4*D*, *middle panel*). A 2-fold molar excess of either IL-6 AU-rich fragment or apoB RNA was sufficient to displace 50% of the bound IL-6 AU-rich probe. By contrast, a non-AU cold RNA competitor failed to disrupt ACF-IL-6 RNA binding (Fig. 4*D*, *bottom*). These findings are summarized and presented quantitatively in the adjacent panel of Fig. 4*D*.

As further evidence that ACF binds IL-6 RNA, we verified *in vivo* protein RNA interaction following UV cross-linking and immunoprecipitation from RAW cells (Fig. 4*E*). By way of a positive control, we subjected murine liver extracts to the same protocol to demonstrate apoB coimmunoprecipitation (Fig. 4*E*), with albumin as a nonspecific control (Fig. 4*E*). These findings collectively indicate that ACF binds IL-6 RNA with similar affinity to that for apoB RNA and provide a plausible foundation for examining the functional consequences of this interaction on mRNA stability. We also determined that deletions in ACF, particularly in RRM 2 and 3, which were previously demonstrated to reduce or eliminate binding to apoB RNA (6, 22), also impair binding to IL-6 (Fig. 4*F*), but that deletion of the putative double-stranded RNA binding domain or elimination of the carboxyl terminus of ACF distal to the RRMs do not impair ACF binding to IL-6 (Fig. 4*F*).

IL-6 mRNA Turnover Is Accelerated in Kupffer Cells from $Acf^{+/-}$ Mice—To examine the role of ACF as a physiological regulator of IL-6 gene expression and specifically its role in regulating mRNA stability, we turned initially to an examination of the role of the AU-rich region of IL-6 in conferring instability to a stable reporter (luciferase) mRNA in HepG2 cells containing differing levels of ACF. However, our results were inconclusive (data not shown), prompting us to undertake studies in primary cells from wild-type and $Acf^{+/-}$ mice. Studies in MEFs revealed a significant baseline reduction in IL-6 mRNA abundance in cells isolated from $Acf^{+/-}$ mice (Fig. 5*A*, *left panel*), although there was a comparable, ~5.7–7.5-fold induction following a 24-h IL-1β treatment in both genotypes (Fig. 5*A*). Studies of IL-6 mRNA decay (using actinomycin D) in MEFs from the different genotypes following IL-1β stimulation, however, revealed indistinguishable kinetics (data not shown). However, following a 24-h incubation with IL-1β, with washes and subsequent reincubation in control medium, the rate of decline of IL-6 mRNA showed a trend to reduced abundance in cells from $Acf^{+/-}$ mice at all time points, reaching statistical significance at 15 h (Fig. 5*A*, *right panel*). These findings again suggest the possibility that IL-6 RNA expression is attenuated in cells from $Acf^{+/-}$ mice. To more directly understand the functional consequences of *Acf* haploinsufficiency on IL-6 mRNA turnover *in vivo*, we then turned to isolated KCs that were stimulated for 1 h with LPS, washed, and then incubated with actinomycin D. The findings show a significant reduction in residual IL-6 mRNA in KCs from $Acf^{+/-}$ mice at 4 and 6 h (Fig. 5*B*). Taken together, these findings demonstrate that ACF binds to the AU-rich region of IL-6 3′-UTR *in vitro* and confers stability to IL-6 mRNA in primary KCs cells, providing a mechanism to account for the loss-of-function phenotype observed in $Acf^{+/-}$ mice.

FIGURE 4. **Characteristics of 3′-UTR of murine IL-6 mRNA and binding activity of ACF.** *A*, the 3′-UTR of murine IL-6 contains 5 copies of the consensus sequence AUUUA, indicated as *asterisks*. The primary sequence of a 128-nt motif surrounding the AUUUA motifs is shown. Numbering begins with the first nucleotide of the 3′-UTR of IL-6 mRNA. ARE-1 extends from nucleotides 126 to 151. ARE-2 extends from nucleotides 160 to 191. Several IL-6 3′-UTR RNA templates were constructed. The 128-nt AU-rich template contains the proximal 4 AUUUA motifs. Mutants 1 and 2 contain point mutations, respectively, in the first two and last two AUUUA motifs. All the point mutations substituted the A and U nucleotides for C and G ("Materials and Methods"). *B*, *left panel*, *in vitro* transcribed radiolabeled IL-6 full-length (*FL*) 3′-UTR was incubated with 25 ng of recombinant ACF and subjected to UV cross-linking. The cross-linked products were analyzed by SDS-10% PAGE. *Right panel*, determination of ACF binding affinity to IL-6 full-length 3′-UTR. Increasing amounts of recombinant ACF were incubated with radiolabeled IL-6 full-length 3′-UTR probe (see "Materials and Methods"). The bound RNA was quantitated after binding to nitrocellulose filters. The apparent K_d was calculated as the concentration of ACF required to retain 50% of the maximum bound RNA. Data represent the mean ± S.E. from 3 separate assays in which each point represents triplicate determinations. *C*, recombinant ACF was incubated for 15 min with *in vitro* transcribed AU-rich, mutant 1, mutant 2, or a non-AU template (p21 coding region) of identical size. After UV cross-linking, the samples were analyzed on SDS-10% PAGE. Mutation of the two proximal AUUUA motifs abrogates ACF interaction with IL-6 AU-rich RNA (*lanes 3* and *4*), whereas mutation of the distal two AUUUA motifs do not affect ACF binding to the RNA probe (*lanes 5* and *6*). This is representative of at least 3 separate experiments. *D*, *left panel*, increasing molar excess of unlabeled (cold) IL-6 AU-rich RNA (*top*) or unlabeled (cold) apoB RNA (*middle*) were added to the radiolabeled IL-6 AU-rich RNA probe in the reaction mixture and are shown to compete out ACF binding to the IL-6 AU-rich template with similar efficiency (2–3-fold molar excess). *Bottom left panel*, increasing excess molar concentration of unlabeled non-AU RNA was added to labeled IL-6 AU-rich RNA and is shown to compete out ACF binding with ~50-fold molar excess. *Right panel*, quantitative representation of UV cross-link binding competition from the *left panels*. The data represent mean ± S.E. ($n = 3$–5 separate experiments per condition). *E*, *in vivo* CLIP reveals ACF-IL-6 interaction. After *in vivo* cross-linking, LPS-stimulated macrophage (RAW 264.3) cell extracts were incubated with either unrelated rabbit IgG (*control Ab*) or anti-ACF antibody. The coimmunoprecipitated RNAs were extracted from the immune complexes and used as template for reverse transcription-PCR using primers specific for IL-6. The PCR products were separated on a 1% agarose gel. *Lane 1* shows IL-6 mRNA in the crude cellular extract before immunoprecipitation. The position of the IL-6 PCR product is indicated by the *arrow* on the *right*. Molecular weights (kb) are shown on the *left*. Similarly, ACF is shown to bind apoB RNA, its canonical RNA template (*middle panel*), in a CLIP assay from mouse liver but fails to interact with a non-AU rich RNA (albumin) (*lower panel*). This is representative of two independent assays. *F*, determination of ACF functional domains required for binding to IL-6 mRNA. *Top panel*, schematic representation of ACF functional domains (6). The three RRM and the putative double-stranded RNA binding domain (*dsRBD*) are shown. *Bottom panel*, individual recombinant ACF mutants (10 ng) were incubated with radiolabeled IL-6 AU-rich template, cross-linked, and analyzed by SDS-10% PAGE. ACF interaction with IL-6 mRNA is dependent on the presence of RRM2 and RRM3 as shown by the lack of cross-link of Δ[RRM2] and Δ[RRM1–3] mutants (*lanes 3* and *4*).

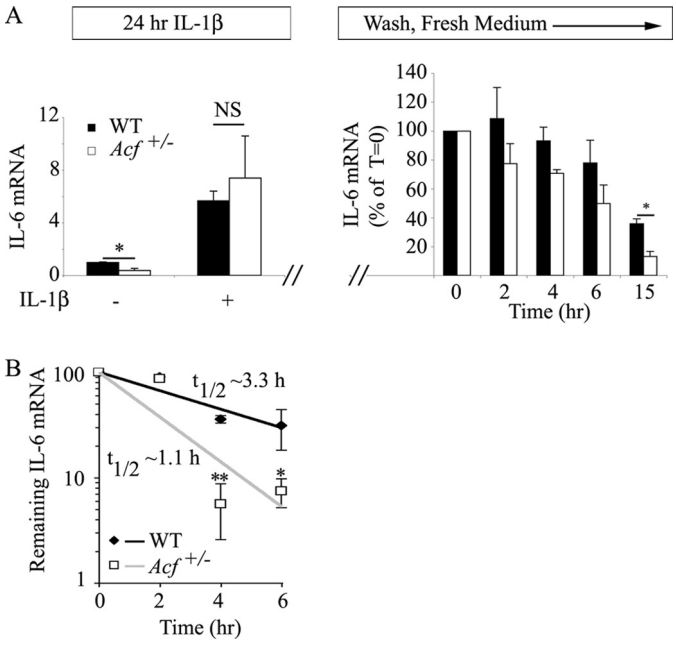

FIGURE 5. **ACF stabilizes IL-6 mRNA.** *A*, IL-6 mRNA steady state in MEFs. WT and $Acf^{+/-}$ MEFs were incubated in the presence of 1 ng/ml of IL-1β for 24 h. Total RNA was isolated from two independent preparations of MEFs. Baseline IL-6 mRNA was significantly (*, $p = 0.018$) lower in MEFs from $Acf^{+/-}$ mice, but both genotypes responded to IL-1β administration with a 5.7–7.4-fold increase in IL-6 mRNA in WT and $Acf^{+/-}$ mice, respectively. In a separate series of studies, following 1 ng/ml of IL-1β incubation for 24 h, MEFs were subjected to 2 washes with PBS, subsequently maintained in normal growth medium, and total RNA isolated at the indicated time points. IL-6 mRNA levels were determined by quantitative reverse transcription-PCR and normalized to glyceraldehyde-3-phosphate dehydrogenase. Data represent mean ± S.E. from 4 independent assays per genotype (*, $p = 0.033$). *B*, KCs were isolated from WT and $Acf^{+/-}$ mice and plated at 4×10^5 cells per well in a 12-well plate. Following an overnight culture at 37 °C, medium was changed and supplemented with LPS (final concentration 500 ng/ml) for 1 h. Conditioned medium was collected, fresh medium containing actinomycin D (Act D) (10 μg/ml) was added, and RNA was harvested at the indicated time points. IL-6 mRNA levels were determined by quantitative reverse transcription-PCR and normalized to glyceraldehyde-3-phosphate dehydrogenase mRNA. The $t_{1/2}$ of IL-6 mRNA was 1.1 ± 0.14 h in $Acf^{+/-}$ KCs *versus* 3.3 ± 0.44 h in WT KCs. Data represent the mean ± S.E. from three independent experiments per genotype. Each experiment was performed with KCs isolated from three to four mice. *, $p = 0.033$; **, $p = 0.0069$.

DISCUSSION

The central findings of this report are that ACF, the RNA binding subunit of the mammalian C to U RNA editing holoenzyme, demonstrates high affinity binding to an AU-rich region in IL-6 3′-UTR with functional consequences for post-transcriptional regulation of IL-6 gene expression and the response of $Acf^{+/-}$ mice to PH. We showed that ACF binds with high affinity to a conserved AU-rich sequence, with a K_d similar to that previously established for its canonical target, apoB mRNA. The attenuated increase in IL-6 mRNA abundance in the regenerating liver of $Acf^{+/-}$ mice is consistent with decreased mRNA stabilization resulting from reduced levels of ACF in KCs. The accompanying reduction in IL-6 mRNA stability and decreased IL-6 secretion from KCs likely contributes to the reduced hepatic regeneration observed following PH. These findings considered together suggest that ACF functions to modulate ARE-dependent decay of the IL-6 transcript in the priming phase of hepatic regeneration. Several elements of these conclusions merit additional discussion.

ACF is the RNA binding component of the apoB RNA editing enzyme and functions both to bind an AU-rich region of the nuclear apoB transcript and also to anchor and position the dimeric RNA-specific cytidine deaminase Apobec-1 into an optimal configuration for C to U deamination of the targeted base at position 6666 (4, 23–25). Structural studies using nuclear magnetic resonance demonstrated that ACF exhibited greater binding affinity for apoB than did Apobec-1 and suggested that increasing concentrations of ACF restricts the RNA binding of Apobec-1 and promotes site-specific C to U editing (25). That said, an apoB RNA editing-independent function for ACF seems plausible because ACF binds to apoB mRNA in human liver-derived HepG2 hepatoma cells, which do not express Apobec-1 and which are not competent to edit apoB mRNA (22, 26, 27) and ACF is widely expressed in human and murine tissues, including some that do not even express apoB RNA (4, 7, 28). Accordingly, these findings establish in principle the possibility that ACF exerts a role in mRNA metabolism beyond its role in apoB RNA editing. The current findings extend this possibility by demonstrating that recombinant ACF binds a 128-nt region of the IL-6 3′-UTR at high affinity and can be competitively displaced by either excess of unlabeled IL-6 itself or unlabeled apoB RNA. In our hands, the binding affinity of ACF for IL-6 and apoB RNA were quite similar (100–200 nM) but lower than the values for apoB reported by Mehta and Driscoll (22) (*i.e.* ~8 nM). However, those authors used a different RNA template (baboon apoB RNA *versus* rat apoB RNA in the current studies), which may account for some of the discrepancy in absolute binding affinities although further study will be required to determine whether species differences in the conserved regions of these templates indeed accounts for the differences observed. Nevertheless, setting aside the quantitative values predicted for RNA binding affinity, our findings demonstrate that ACF binds with comparable affinity to either apoB or IL-6 RNA. It is also worth pointing out that the functional domains in ACF required for IL-6 RNA binding seem to be the same as those described for apoB RNA, namely the three RRMs, predominantly RRM 2 and 3, domains that overlap with its heteromeric protein-protein interaction (6, 22).

Modeling predictions for the AU-rich region of apoB RNA flanking the edited base suggest a stem-loop structure (29) and our preliminary analyses suggest that the 128-nt region of IL-6 RNA also adopts similarly stable stem-loop configurations.[3] Further studies will be required to formally address the possibility that ACF binds a structural motif in the IL-6 3′-UTR rather than a linear AU-rich sequence. This possibility is relevant in relation to the findings of Paschoud and colleagues (13) who demonstrated that AUF1 binds to a region in the human IL-6 3′-UTR comprising two distinct elements but were unable to resolve unambiguously whether sequence alone or the structural context of this binding sequence was the crucial factor. These authors further demonstrated that AUF1 promoted degradation of an IL-6 3′-UTR reporter mRNA through interactions within the L-site (nucleotides 848 to 871 of the human IL-6 3′-UTR) that overlaps with the 128-nt region identified in

[3] V. Blanc, K. Sessa, and N. O. Davidson, unpublished observations.

the current findings as the ACF binding site (13). These findings, although extrapolated from human to murine IL-6 3′-UTR, raise the intriguing possibility that combinatorial interactions of RNA-binding proteins within the 3′-UTR of IL-6 may in turn function to modulate IL-6 mRNA stability. Extending this possibility more broadly, it is tempting to speculate that the range of RNA targets to which ACF binds is functionally constrained by both its cell-specific context (*i.e.* both cell type and subcellular localization) as well as protein-protein interactions. This implication carries significance for the biological functions of ACF by analogy with other RNA-binding proteins, including tristetraprolin, which modulates interferon γ mRNA decay in T cells (30) and also members of the ELAV/Hu family such as HuR that contain similar RRM domains, which are ubiquitously expressed and (like ACF) shuttle between the nucleus and cytoplasm and function to stabilize AU-rich target RNAs (1).

If ACF plays a role in stabilizing IL-6 mRNA, why is it that alterations in IL-6 mRNA stability were found in KCs but not MEFs prepared from $Acf^{+/-}$ mice? Among the possibilities that we are continuing to explore is that the expression level of ACF as well as the stoichiometry of other AU-rich RNA-binding proteins (including AUF-1, HuR, and others) each plays a crucial role. Preliminary observations suggest that MEFs express extremely low levels of ACF in comparison to the levels observed in KCs[4] raising the testable hypothesis that a conditional gain-of-function may be elicited in MEFs in regard to IL-6 mRNA stability. Future studies will be required to formally examine this possibility.

Our findings suggest that ACF participates in the post-transcriptional regulation of IL-6, which in turn functions as part of an elaborate network to orchestrate the early phase of liver regeneration following PH. This suggestion is based on the findings of delayed liver mass restitution and decreased DNA synthesis, coupled with decreased serum IL-6 and decreased IL-6 mRNA and protein secretion from KCs. These findings were somewhat unexpected because we had predicted *a priori* that any liver growth phenotype would most likely reflect *Acf* haploinsufficiency and loss-of-function within hepatocytes (the dominant site of ACF expression) rather than non-parenchymal cells. Our findings do not preclude alterations in the abundance or stability of other hepatocyte RNAs in $Acf^{+/-}$ mice but suggest that the phenotype observed in response to PH is at least in part accounted for by decreased IL-6 production from KCs rather than hepatocytes (11). This suggestion is consistent with earlier reports demonstrating the importance of IL-6 in liver regeneration. There is abundant evidence, for example, that the priming phase of liver regeneration is regulated through diverse signaling pathways including both innate and adaptive immune pathways (31), inflammatory signaling cascades and cytokines (such as tumor necrosis factor α) with IL-6 playing a central role (12, 32–34) (reviewed in Ref. 11). Nevertheless, the precise role of IL-6 in liver regeneration is still incompletely resolved and it is clear that there is redundancy in the cytokine pathway because oncostatin M (another member of the IL-6 family) (35) or stem cell factor (36) can each rescue the phenotype of defective liver regeneration in $IL\text{-}6^{-/-}$ mice. It remains to be demonstrated just how these various signaling pathways intersect with ACF regulation of IL-6 expression and these questions will be the focus of ongoing study. In this context, a major objective is to extend this loss-of-function phenotype in an *in vivo* model with tissue- and cell-specific *Acf* deletion. These and other objectives will be the focus of future reports.

[4] V. Blanc and N. O. Davidson, unpublished observations.

REFERENCES

1. Glisovic, T., Bachorik, J. L., Yong, J., and Dreyfuss, G. (2008) *FEBS Lett.* **582,** 1977–1986
2. Blanc, V., and Davidson, N. O. (2003) *J. Biol. Chem.* **278,** 1395–1398
3. Teng, B., Burant, C. F., and Davidson, N. O. (1993) *Science* **260,** 1816–1819
4. Mehta, A., Kinter, M. T., Sherman, N. E., and Driscoll, D. M. (2000) *Mol. Cell. Biol.* **20,** 1846–1854
5. Lellek, H., Kirsten, R., Diehl, I., Apostel, F., Buck, F., and Greeve, J. (2000) *J. Biol. Chem.* **275,** 19848–19856
6. Blanc, V., Henderson, J. O., Kennedy, S., and Davidson, N. O. (2001) *J. Biol. Chem.* **276,** 46386–46393
7. Henderson, J. O., Blanc, V., and Davidson, N. O. (2001) *Biochim. Biophys. Acta* **1522,** 22–30
8. Blanc, V., Henderson, J. O., Newberry, E. P., Kennedy, S., Luo, J., and Davidson, N. O. (2005) *Mol. Cell. Biol.* **25,** 7260–7269
9. Michalopoulos, G. K. (2007) *J. Cell. Physiol.* **213,** 286–300
10. Taub, R. (2004) *Nat. Rev. Mol. Cell Biol.* **5,** 836–847
11. Fausto, N., Campbell, J. S., and Riehle, K. J. (2006) *Hepatology* **43,** S45–53
12. Cressman, D. E., Greenbaum, L. E., DeAngelis, R. A., Ciliberto, G., Furth, E. E., Poli, V., and Taub, R. (1996) *Science* **274,** 1379–1383
13. Paschoud, S., Dogar, A. M., Kuntz, C., Grisoni-Neupert, B., Richman, L., and Kühn, L. C. (2006) *Mol. Cell. Biol.* **26,** 8228–8241
14. Newberry, E. P., Kennedy, S. M., Xie, Y., Luo, J., Stanley, S. E., Semenkovich, C. F., Crooke, R. M., Graham, M. J., and Davidson, N. O. (2008) *Hepatology* **48,** 1097–1105
15. Smedsrød, B., and Pertoft, H. (1985) *J. Leukocyte Biol.* **38,** 213–230
16. Hoyle, G. W., and Hill, R. L. (1991) *J. Biol. Chem.* **266,** 1850–1857
17. Takahashi, K., and Yamanaka, S. (2006) *Cell* **126,** 663–676
18. Yatsenko, O. P., Filipenko, M. L., Khrapov, E. A., Voronina, E. N., Sennikov, S. V., and Kozlov, V. A. (2004) *Bull. Exp. Biol. Med.* **138,** 73–76
19. Ule, J., Jensen, K., Mele, A., and Darnell, R. B. (2005) *Methods* **37,** 376–386
20. Bihl, M. P., Heinimann, K., Rüdiger, J. J., Eickelberg, O., Perruchoud, A. P., Tamm, M., and Roth, M. (2002) *Am. J. Respir. Cell Mol. Biol.* **27,** 48–56
21. Bultinck, J., Brouckaert, P., and Cauwels, A. (2006) *Cytokine* **36,** 160–166
22. Mehta, A., and Driscoll, D. M. (2002) *RNA* **8,** 69–82
23. Chester, A., Weinreb, V., Carter, C. W., Jr., and Navaratnam, N. (2004) *RNA* **10,** 1399–1411
24. Blanc, V., Navaratnam, N., Henderson, J. O., Anant, S., Kennedy, S., Jarmuz, A., Scott, J., and Davidson, N. O. (2001) *J. Biol. Chem.* **276,** 10272–10283
25. Maris, C., Masse, J., Chester, A., Navaratnam, N., and Allain, F. H. (2005) *RNA* **11,** 173–186
26. Greeve, J., Altkemper, I., Dieterich, J. H., Greten, H., and Windler, E. (1993) *J. Lipid Res.* **34,** 1367–1383
27. Giannoni, F., Bonen, D. K., Funahashi, T., Hadjiagapiou, C., Burant, C. F., and Davidson, N. O. (1994) *J. Biol. Chem.* **269,** 5932–5936
28. Sowden, M. P., Lehmann, D. M., Lin, X., Smith, C. O., and Smith, H. C. (2004) *J. Biol. Chem.* **279,** 197–206
29. Anant, S., and Davidson, N. O. (2000) *Mol. Cell. Biol.* **20,** 1982–1992
30. Ogilvie, R. L., Sternjohn, J. R., Rattenbacher, B., Vlasova, I. A., Williams, D. A., Hau, H. H., Blackshear, P. J., and Bohjanen, P. R. (2009) *J. Biol. Chem.* **284,** 11216–11223

31. Tumanov, A. V., Koroleva, E. P., Christiansen, P. A., Khan, M. A., Ruddy, M. J., Burnette, B., Papa, S., Franzoso, G., Nedospasov, S. A., Fu, Y. X., and Anders, R. A. (2009) *Gastroenterology* **136,** 694–704.e4
32. Wuestefeld, T., Klein, C., Streetz, K. L., Betz, U., Lauber, J., Buer, J., Manns, M. P., Müller, W., and Trautwein, C. (2003) *J. Biol. Chem.* **278,** 11281–11288
33. Zimmers, T. A., Pierce, R. H., McKillop, I. H., and Koniaris, L. G. (2003) *Hepatology* **38,** 1590–1591; author reply 1591
34. Blindenbacher, A., Wang, X., Langer, I., Savino, R., Terracciano, L., and Heim, M. H. (2003) *Hepatology* **38,** 674–682
35. Nakamura, K., Nonaka, H., Saito, H., Tanaka, M., and Miyajima, A. (2004) *Hepatology* **39,** 635–644
36. Ren, X., Hogaboam, C., Carpenter, A., and Colletti, L. (2003) *J. Clin. Invest.* **112,** 1407–1418